Radio-frequency-heating capability of silica-coated manganese ferrite nanoparticles

Qiu Qing-Wei(邱庆伟)[a)†], Xu Xiao-Wen(徐晓文)[a)], He Mang(何 芒)[a)], and Zhang Hong-Wang(张洪旺)[b)]

[a)] *School of Information and Electronics, Beijing Institute of Technology, Beijing* 100081, *China*

[b)] *Department of Physics, University at Buffalo, SUNY, Buffalo, New York* 14260, *USA*

(Received 21 January 2015; revised manuscript received 5 February 2015; published online 10 April 2015)

$MnFe_2O_4$ nanoparticles (NPs) with various sizes and tight size-distribution were synthesized by a chemical solution-phase method. The as-synthesized NPs were coated with a silica shell of 4 nm–5 nm in thickness, enabling the water-solubility and biocompatibility of the NPs. The $MnFe_2O_4$ NPs with a size of less than 18 nm exhibit superparamagnetic behavior with high saturated magnetization. The capacity of the heat production was enhanced by increasing particle sizes and radio frequency (RF) field strengths. $MnFe_2O_4/SiO_2$ NPs with 18-nm magnetic cores showed the highest heat-generation ability under an RF field. These $MnFe_2O_4/SiO_2$ NPs have great potentiality to cancer treatments, controlled drug releases, and remote controls of single cell functions.

Keywords: manganese ferrite, magnetic nanoparticles, silica coating, hyperthermia

PACS: 75.47.Lx, 75.75.–c **DOI:** 10.1088/1674-1056/24/6/067503

1. Introduction

In the past few years, the applications of magnetic nanoparticles (NPs) have expanded rapidly from just high-density storage media to a variety of technologies. In particular, their potential biomedical applications have drawn great attention, such as targeted drug delivery, biological separation, contrast agent in magnetic resonance imaging (MRI), and hyperthermia cancer treatment.[1–9] The latter one, magnetic hyperthermia, employs a novel therapeutic concept to kill tumor cells, first proposed by Gilchrist in 1957.[10] This treatment involves delivering magnetic NPs to the target tissue and then applying an alternative magnetic field of sufficient frequency and amplitude to cause the NPs to heat. Ferrite magnetic NPs are often selected in magnetic hyperthermia because of their biocompatibility and availability.[11–13] In order to minimize the potential side effects arising in magnetic hyperthermia, ferrite NP should be applied at a low dose as possible, while this dosage can still maintain a sufficient heating source. To satisfy the latter case, magnetic NPs with higher energy transfer efficiency are mostly preferred.[14–17] Therefore, to develop new NPs with sufficient heating ability is of great importance. The heat generation capacity of magnetic NPs under an alternative magnetic field is expressed by the specific absorption rate (SAR). The SAR of NPs is determined by their intrinsic properties, such as magnetization and magnetic anisotropy. High saturated magnetization and moderate anisotropy are suitable for increasing the heating ability of NPs.[18–20]

$MnFe_2O_4$ NPs are chosen to be an ideal candidate for magnetic hyperthermia because it has very high magnetization and stability against oxidation. Magnetic NPs with high productivity and narrow size distribution are usually synthesized by the thermal decomposition method in an organic solvent.[21–23] Thus, these NPs are usually covered by a layer of surfactants (e.g., oleic acid and/or oleylamine), which enable their good dispersability in non-polar solvents. However, to be used in hyperthermal therapy, magnetic NPs are expected to be water-soluble and disperse well in aqueous solution. Therefore, magnetic NPs obtained in the organic-phase are usually coated with various surface layers, such as polymer, silica, or carbon in order to enhance their hydrophilicity. Silica coating has been widely used in biomedical applications because of its excellent biocompatibility, high stability, nontoxicity, and easy functionalization.[24–26] Herein, we report our studies on the synthesis of size-tunable $MnFe_2O_4$ NPs coated with a silica shell and their heating efficiency under a radio frequency (RF) field in a solution. Our results show that the SAR value of $MnFe_2O_4$/silica core/shell NPs is strongly dependent on the size of magnetic cores and the strength of applied magnetic fields.

2. Experimental methods

Monodisperse $MnFe_2O_4$ NPs were synthesized by the thermal decomposition method in an organic phase.[21,22] The silica shells were coated on the hydrophobic $MnFe_2O_4$ NPs via a reverse microemulsion method.[24,26] The size and morphology of the NPs were characterized by a Hitachi H7650 (120 kV) transmission electron microscope (TEM). The composition was investigated by energy dispersive x-ray spectroscopy (EDX). The magnetic hysteresis loops were measured using a Quantum Design Physical Property Measure-

†Corresponding author. E-mail: qiuqingwei@bit.edu.cn

© 2015 Chinese Physical Society and IOP Publishing Ltd

ment System Model 6000. Hyperthermia performance of $MnFe_2O_4$ NPs was investigated by a HYPER5 machine fabricated by the MSI Company under a radio frequency field of 400 kHz.

3. Results and discussion

The sizes of $MnFe_2O_4$ NPs were tuned by varying the experimental conditions. Figure 1 shows the TEM images of the as-synthesized $MnFe_2O_4$ NPs with sizes of 7, 12, and 18 nm. The 7-nm and 12-nm $MnFe_2O_4$ NPs were obtained directly through thermal decomposition of iron acetylacetonate and manganese acetylacetonate with surfactants in a high-boiling point organic solvent, while 18-nm $MnFe_2O_4$ NPs were produced by a seed-mediated growth method. An energy dispersive x-ray (EDX) elemental analysis of the $MnFe_2O_4$ NPs was performed and the atomic composition is shown in Table 1. EDX results revealed that the composition of NPs is very close to the stoichiometry of $MnFe_2O_4$. A thin layer of silica coating on the magnetic NPs was performed by the reverse microemulsion method. The silica-coated NPs dispersed well in an aqueous solution and are stable for months without agglomeration. The TEM images of $MnFe_2O_4/SiO_2$ with different magnetic cores are shown in Figs. 1(d)–1(f). It was observed that the silica shells were 4 nm–5 nm in thickness, and no free silica particles appeared.

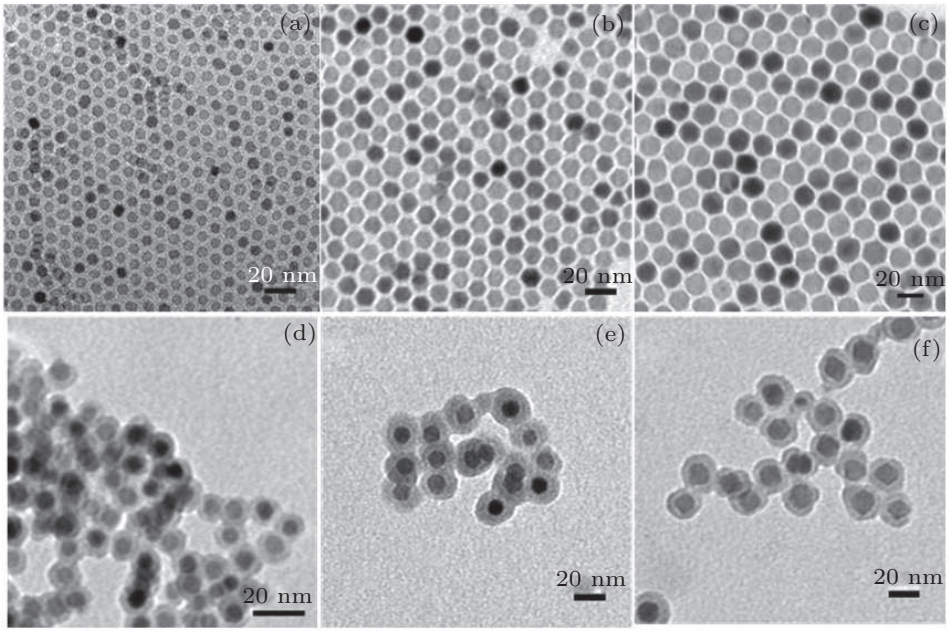


Fig. 1. TEM images of $MnFe_2O_4$ nanoparticles of (a) 7 nm, (b) 12 nm, and (c) 18 nm; and $MnFe_2O_4/SiO_2$ nanoparticles using (d) 7 nm, (e) 12-nm, and (f) 18-nm $MnFe_2O_4$ nanoparticles as seeds.

Table 1. The composition of $MnFe_2O_4$ NPs examined by EDX.

Samples	Mn/at.%	Fe/at.%	O/at.%
7 nm	13.9	27.5	56.8
12 nm	14.58	28.3	57.1
18 nm	14.68	27.9	57.5

The magnetic hysteresis loops of uncoated $MnFe_2O_4$ NPs were demonstrated in Fig. 2. All the $MnFe_2O_4$ NPs are superparamagnetic at both 5 K and 300 K, and larger NPs show higher saturation magnetization (M_S). As the particles size was increased from 7 nm to 18 nm, the saturated magnetization at 300 K rose from 65 emu/g to 80 emu/g. The M_S value of 18-nm $MnFe_2O_4$ NPs was only a little less than that of bulk $MnFe_2O_4$ (90 emu/g), which suggested the excellent crystallinity of the NPs. The slightly reduced magnetization may be due to surface spin disorder.

To demonstrate the heating capability, the aqueous solutions of $MnFe_2O_4/SiO_2$ NPs (10-mg $MnFe_2O_4$ per mL) were placed under an RF field of 400 kHz. The temperature of the solution was monitored by an optic fiber probe. The temperature-rising curves measured in the aqueous suspensions of $MnFe_2O_4/SiO_2$ NPs were described in Fig. 3. The contribution from pure water under the same conditions was also measured and deducted. It was shown that 7-nm $MnFe_2O_4/SiO_2$ NPs were unable to be heated even though the RF strength reached 320 Gs (1 Gs = 10^{-4} T). On the other side, $MnFe_2O_4/SiO_2$ NPs with the core sizes of 12 and 18 nm exhibited a heat generation ability under a RF field. $MnFe_2O_4/SiO_2$ NPs with 18-nm magnetic core showed a much higher heating efficiency than those with 12-nm cores. When the core sizes were larger than 18 nm, $MnFe_2O_4/SiO_2$ NPs tend to aggregate in the solution due to the magnetic interaction. Therefore, they

are excluded from further characterization in this work. It was also apparent that the heating capability of $MnFe_2O_4/SiO_2$ NPs was enhanced by increasing the magnitude of the RF fields. The temperature rise of the aqueous suspensions containing $MnFe_2O_4/SiO_2$ NPs should be dose-dependent. Therefore, it is necessary to measure the temperature-rising curve of the aqueous suspensions with different concentration of $MnFe_2O_4/SiO_2$ NPs, as shown in Fig. 4. It is found that the temperature rise of the aqueous suspensions is strongly dependent on the concentration of $MnFe_2O_4/SiO_2$ NPs.

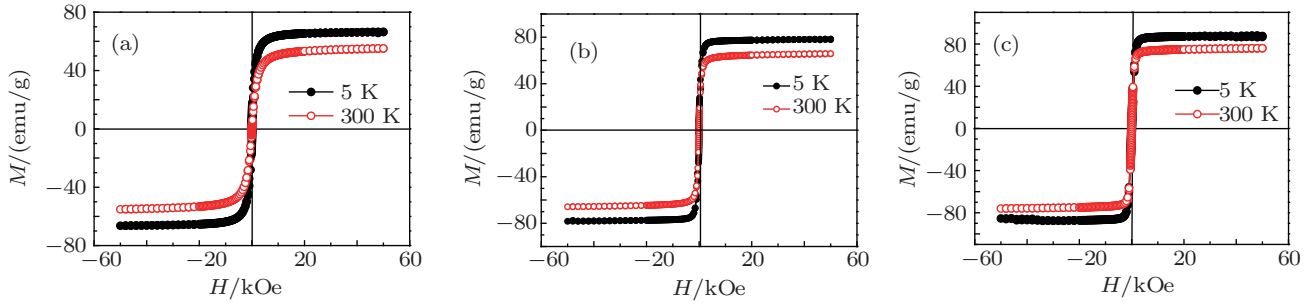


Fig. 2. (color online) The magnetic hysteresis loops of as-synthesized $MnFe_2O_4$ nanoparticles of (a) 7 nm, (b) 12 nm, and (c) 18 nm, measured at 5 K and 300 K. The unit 1 Oe = 79.5775 A·m^{-1}.

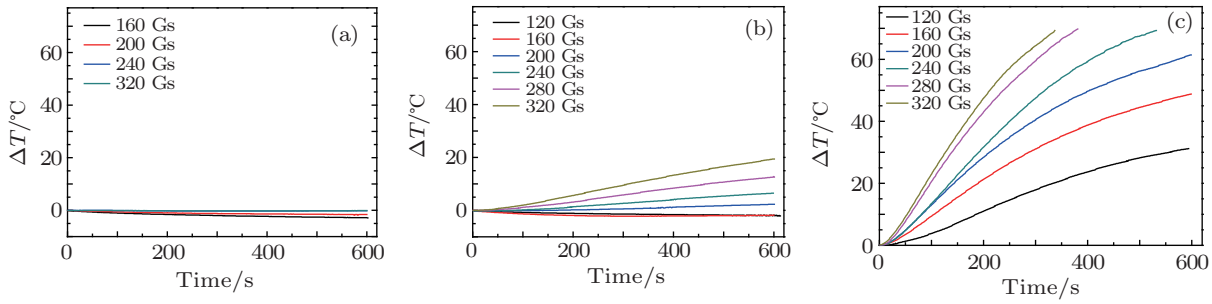


Fig. 3. (color online) Temperature rise measured in the aqueous suspensions of $MnFe_2O_4/SiO_2$ nanoparticles with different core sizes of (a) 7 nm, (b) 12 nm, and (c) 18 nm under the RF field of 400 kHz with different field magnitudes.

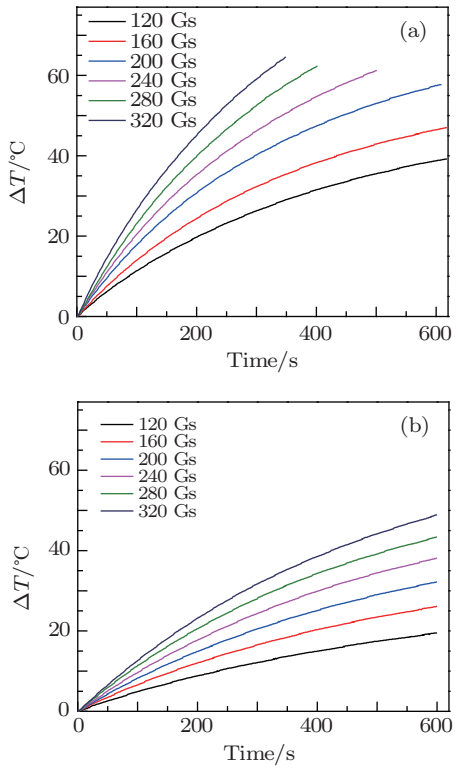


Fig. 4. (color online) Temperature rise measured in the aqueous suspensions (a) 5-mg $MnFe_2O_4$ per mL and (b) 2.5-mg $MnFe_2O_4$ per mL of $MnFe_2O_4/SiO_2$ nanoparticles with 18-nm magnetic core.

The physical mechanism of heating for superparamagnetic fluid was proposed by Rosensweig.[27] The heat generation of superparamagnetic fluid results from Néel and Brown relaxation processes. The Brown relaxation mechanism is related to the mechanical movement of NPs in the fluid, while Néel relaxation is attributed to the relaxation of magnetic domain rotation of superparamagnetic NPs. The loss power due to magnetic relaxation can be calculated according to

$$P = \mu_0 \pi \chi_0 H^2 f \frac{\omega\tau}{1+(\omega\tau)^2}, \tag{1}$$

where μ_0 is the permeability of free space, χ_0 is the DC susceptibility, H is the magnitude of the RF field, f is the frequency of the RF field ($f = \omega/2\pi$), and τ is the relaxation time. Equation (1) indicates that the heating ability of magnetic NPs is improved with the enhancement of the RF field. This is consistent with our results. For superparamagnetic NPs with low anisotropy, such as $MnFe_2O_4$ NPs, the field- and temperature-dependent magnetization obeys the Langevin function, from which we can derive χ_0:

$$M = M_S L\left(\frac{M_S V H}{k_B T}\right) \approx \frac{1}{3}\frac{M_S^2 V H}{k_B T}, \tag{2}$$

$$\chi_0 = \frac{\mathrm{d}M}{\mathrm{d}H} \approx \frac{1}{3}\frac{M_S^2 V}{k_B T}. \tag{3}$$

Equation (3) demonstrates that χ_0 is proportional to the saturated magnetization and NP size. Bigger $MnFe_2O_4$ NPs apparently own a larger volume, leading to higher χ_0. Furthermore our magnetic measurements have already shown that larger NPs exhibited higher M_S. Therefore, the heating capability of $MnFe_2O_4$ NPs was improved by increasing their sizes. This well explains our observations that the core/shell NPs with 7-nm cores can hardly heat, while those with 18-nm cores own the highest heating efficiency.

We then obtained the SAR values of the $MnFe_2O_4$/silica NPs in solution according to the following equation:

$$\mathrm{SAR} = \frac{C}{m}\frac{\mathrm{d}T}{\mathrm{d}t}, \tag{4}$$

where C is the specific heat capacity of water per unit volume and m is the concentration of NPs in the solution. The slope of the curve $\mathrm{d}T/\mathrm{d}t$ was calculated by taking the first few seconds into account. The SAR has the unit of Watts per mass of magnetic nanoparticles (W/g). The SAR values of the 12- and 18-nm $MnFe_2O_4$ NPs calculated from Figs. 3(b) and 3(c) were listed in Table 2. It is noted that the SAR of the core/shell NPs with 18-nm cores reached a value of 336 W/g under the RF field of 400 kHz and 320 Gs.

Table 2. Specific absorption rates (SAR) of $MnFe_2O_4/SiO_2$ NPs with core size of 12 nm and 18 nm. SAR values are given per gram of magnetic core material.

NP core size/nm	RF field/Gs	SAR/(W/g)
18	120	103
18	160	152
18	200	213
18	240	247
18	280	302
18	320	336
12	280	26
12	320	67

4. Conclusions

In summary, we have synthesized $MnFe_2O_4/SiO_2$ core/shell NPs with tunable $MnFe_2O_4$ core sizes ranging from 7 nm to 18 nm. The NPs with 7-nm magnetic cores cannot be heated in RF field at 400 kHz. However, those with 12-nm and 18-nm cores can generate heat in RF field. The heating capability of $MnFe_2O_4/SiO_2$ NPs was improved by the increase of RF field strength. Larger particles showed higher M_S and χ_0, and consequently exhibited a stronger heating capability. The SAR value of the NPs with 18-nm $MnFe_2O_4$ cores was 336 W/g under a magnetic field of 400 kHz and 320 Gs. With their efficient hyperthermia performance, these magnetic core/shell NPs may have broad applications in nanobiotechnology.

References

[1] Jeong U, Teng X W, Wang Y, Yang H and Xia Y N 2007 *Adv. Mater.* **19** 33
[2] Xu C J and Sun S H 2013 *Adv. Drug. Deliv. Rev.* **65** 732
[3] Sun C, Lee J S H and Zhang M Q 2008 *Adv. Drug. Deliv. Rev.* **60** 1252
[4] Frey N A, Peng S, Cheng K and Sun S H 2009 *Chem. Soc. Rev.* **38** 2532
[5] Jordan A, Wust P, Fahling H, John W, Hinz A and Felix R 1993 *Int. J. Hyperther.* **9** 51
[6] Huang X H, El-Sayed I H, Qian W and El-Sayed M A 2006 *J. Am. Chem. Soc.* **128** 2115
[7] Liu T Y, Hu S H, Liu D M, Chen S Y and Chen I W 2009 *Nano Today* **4** 52
[8] Meffre A, Mehdaoui B, Kelsen V, Fazzini P F, Carrey J, Lachaize S, Respaud M and Chaudret B 2012 *Nano Lett.* **12** 4722
[9] Yang C, Hong Y L and Gao S 2014 *Chin. Phys. B* **23** 057505
[10] Gilchrist R K, Medal R, Shorey W D, Hanselman R C, Parrott J C and Taylor C B 1957 *Ann. Surg.* **146** 596
[11] Hergt R, Dutz S, Muller R and Zeisberger M 2006 *J. Phys.: Condens. Matter* **18** S2919
[12] Gupta A K and Gupta M 2005 *Biomaterials* **26** 3995
[13] Guardia P, Di Corato R, Lartigue L, Wilhelm C, Espinosa A, Garcia-Hernandez M, Gazeau F, Manna L and Pellegrino T 2012 *ACS Nano* **6** 3080
[14] Chen R, Christiansen M G and Anikeeva P 2013 *ACS Nano* **7** 8990
[15] Lee J H, Jang J T, Choi J S, Moon S H, Noh S H, Kim J W, Kim J G, Kim I S, Park K I and Cheon J 2011 *Nat. Nanotechnol.* **6** 418
[16] Mehdaoui B, Meffre A, Carrey J, Lachaize S, Lacroix L M, Gougeon M, Chaudret B and Respaud M 2011 *Adv. Funct. Mater.* **21** 4573
[17] Carrey J, Mehdaoui B and Respaud M 2011 *J. Appl. Phys.* **110** 083921
[18] Habib A H, Ondeck C L, Chaudhary P, Bockstaller M R and McHenry M E 2008 *J. Appl. Phys.* **103** 03A307
[19] Kappiyoor R, Liangruksa M, Ganguly R and Puri I K 2010 *J. Appl. Phys.* **108** 094702
[20] Fortin J P, Wilhelm C, Servais J, Menager C, Bacri J C and Gazeau F 2007 *J. Am. Chem. Soc.* **129** 2628
[21] Sun S H and Zeng H 2002 *J. Am. Chem. Soc.* **124** 8204
[22] Sun S H, Zeng H, Robinson D B, Raoux S, Rice P M, Wang S X and Li G X 2004 *J. Am. Chem. Soc.* **126** 273
[23] Zeng H, Rice P M, Wang S X and Sun S H 2004 *J. Am. Chem. Soc.* **126** 11458
[24] Ding H L, Zhang Y X, Wang S, Xu J M, Xu S C and Li G H 2012 *Chem. Mater.* **24** 4572
[25] Selvan S T, Tan T T and Ying J Y 2005 *Adv. Mater.* **17** 1620
[26] Zhang H, Huang H, He S, Zeng H and Pralle A 2014 *Nanoscale* **6** 13463
[27] Rosensweig R E 2002 *J. Magn. Magn. Mater.* **252** 370